T.Z. Maung, D. Oetomo, M.H. Ang Jr., T.K. Ng, "Kinematics and Dynamics of an Omnidirectional Mobile Platform with Powered Caster Wheels," *International Symposium on Dynamics and Control, Hanoi*, Vietnam, 15-20 September, 2003.

KINEMATICS AND DYNAMICS OF AN OMNIDIRECTIONAL MOBILE PLATFORM WITH POWERED CASTER WHEELS

Maung ThanZaw[†] **Denny Oetomo**[†]
Marcelo H. Ang Jr. **Ng Teck Khim**
National University of Singapore
[†]*Singapore Institute of Manufacturing Technology*

Abstract

Mobile robots with omni-directional motion capabilities are very useful especially in mobile manipulation tasks and tasks in human environment. In this paper, we present the kinematics and dynamics of one class of omni-directional mobile robots that is driven by a 2 axis powered caster wheels with non-intersecting axes of motions (caster wheels with offset). Our derivation approach treats the each caster wheel as a serial manipulator and the entire system as a parallel manipulator generated by several serial manipulator with a common end-effector, following the operational space formulation by Khatib

1 Introduction

Omnidirectional wheeled mobile robots have been an active research area over the past three decades. The advantages over the legged mobile robots are the ease of manufacture, high pay load, high efficiency, and the ability to perform tasks in congested and narrow environment.

There are three types of wheels [1]: the conventional wheels, the omnidirectional wheels, and the ball wheel. The conventional wheels are the wheels that we see everyday, such as those on the cars and trolleys. An omnidirectional wheel is a disk-like wheel with a multitude of conventional wheels mounted on its periphery. The ball wheel is one that's shaped like a ball.

The ball wheel [2, 3] is difficult to implement as it is not possible to place an axel through the ball without sacrificing the usable workspace. It is difficult to transmit power to drive the wheel. There is also the practical need of keeping it robust from collected dust and dirt from the floor. There has been a lot of effort in the development of omnidirectional wheels [4, 5, 6]. Due to multiple number of small rollers on the periphery of the wheel, an undesirable vibration often exists in the motion.

The conventional wheel is probably the simplest and most robust among the designs. However, not all conventional wheels are capable of providing omnidirec-

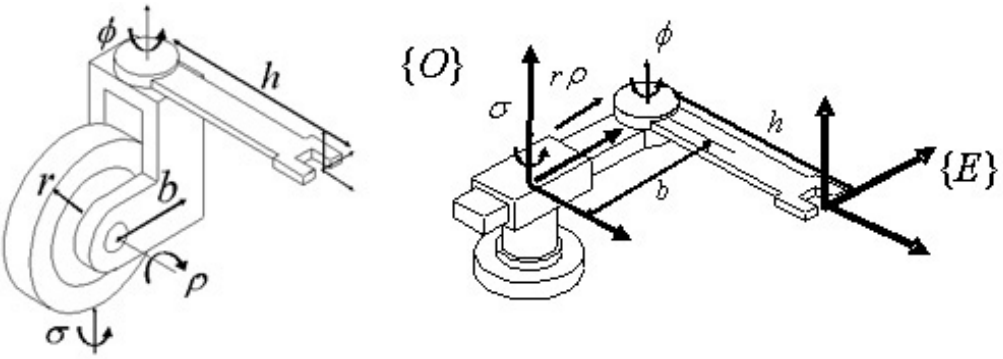

Figure 1: An offset or caster wheel. This design was chosen to provide an omnidirectional motion capability to the mobile platform. Shown in this figure is the instantaneous model of the caster wheel.

tional motion capability [1] [7] [8]. Chosen in our design was an offset wheel or what is often described as caster wheel [9] [10] (see Figure 1). It has been widely accepted that caster design provides full mobility [11].

The kinematics and dynamics of the mechanism is not new [12]. However, our derivation approach follows the conventional methods in treating open chain (serial) and closed chain (parallel) manipulator, by using DH convention, the operational space formulation [13] and the *augmented object model* [14] [15]. The augmented object model was utilised to represent the mobile robot as a system of cooperating manipulators, where each wheel module is modelled a serial manipulator. The objective of the design is to obtain an omnidirectional mobile robot (with 3 DOF motion capability).

2 Kinematics Modelling of a Single Caster Wheel

In the formulation of kinematics model, we treat the wheel module as a serial link manipulator with two revolute joints and one prismatic joint in instantaneous time. The point of wheel contact with the floor is taken as a revolute joint (σ). This is a passive joint with no position feedback, as this is the twist angle between the wheel contact and the floor. With the assumption of no slippage, the forward rolling motion of the wheel is treated as a prismatic joint ($r\rho$) where r is the wheel radius and ρ is the angular displacement is radians. The steering joint is the last revolute joint (ϕ) of the system. See Figure 1.

By instantaneous, we mean that the prismatic joint ($r\rho$) provides an instantaneous linear translation that pushes the end-effector forward with respect to the floor. At the same time, the mechanism has a set length of b (the wheel offset) between the rotation axes of σ and ϕ. The D-H parameter for the single caster wheel modelled as a serial manipulator is shown in Table 1.

The Frame O is an instantaneous frame that is always parallel to the world (absolute) frame, but moves together with the wheel. In other words, it is attached to the contact point between the wheel and the floor.

Table 1: D-H parameters of the single caster wheel

Joint i	α_i	a_i	θ_i	d_i
1	$-\pi/2$	0	σ	0
2	$\pi/2$	0	0	$r\rho$
3	0	0	ϕ	0

The position of the end-effector with respect to Frame O is:

$$ {}^{0}\mathbf{p}_E = \begin{bmatrix} r\rho c_\sigma + hc_{\sigma+\phi} \\ r\rho s_\sigma + hs_{\sigma+\phi} \\ 0 \end{bmatrix} \tag{1} $$

where r is the wheel radius, $c_\sigma = Cos(\sigma)$ and $c_{\sigma+\phi} = Cos(\sigma + \phi)$. The same applies to the sines. The end-effector is located at the center of the mobile base, therefore the length of the second link of the model above is taken as h, where h is the radius of the mobile base.

When differentiated, the position vector $\mathbf{x}$ will provide the velocity vector of the end-effector, or upon rearranging, the Jacobian matrix and the joint velocity vector. Note that when differentiating $r\rho$ with respect to σ and ϕ, it is taken as the constant value of the offset b, which is the real physical distance. However, when differentiating it respect to ρ, it is taken as a variable with respect to time, resulting in $\frac{\delta(r\rho)}{\delta t} = r\dot{\rho}$.

Adding the rotational components (the rotational axes of σ and ϕ) into the Jacobian matrix, we obtain:

$$ {}^{0}\mathbf{J} = \begin{bmatrix} -hs_{\sigma+\phi} - r\rho s_\sigma & rc_\sigma & -hs_{\sigma+\phi} \\ hc_{\sigma+\phi} + r\rho c_\sigma & rs_\sigma & hc_{\sigma+\phi} \\ 1 & 0 & 1 \end{bmatrix} \tag{2} $$

where

$$ \dot{\mathbf{x}} = \begin{pmatrix} \dot{x} \\ \dot{y} \\ \dot{\theta} \end{pmatrix} = \mathbf{J} \begin{pmatrix} \dot{\sigma} \\ \dot{\rho} \\ \dot{\phi} \end{pmatrix} \tag{3} $$

This is the Jacobian matrix with respect to Frame O. Notice that the Jacobian is a function of σ and ϕ. Since σ is not a measurable nor controllable variable, it is desired to have a Jacobian matrix that is not a function of σ. This is obtained by expressing the Jacobian with respect to the end-effector frame (Frame {E} in Figure 1).

To do so, the Jacobian is pre-multiplied by a rotational matrix:

$$ {}^{E}\mathbf{J} = {}^{E}\mathbf{R}_0 . {}^{0}\mathbf{J} \tag{4} $$

where ${}^{E}\mathbf{R}_0$ is a rotation matrix derived from angle $(\sigma + \phi)$.

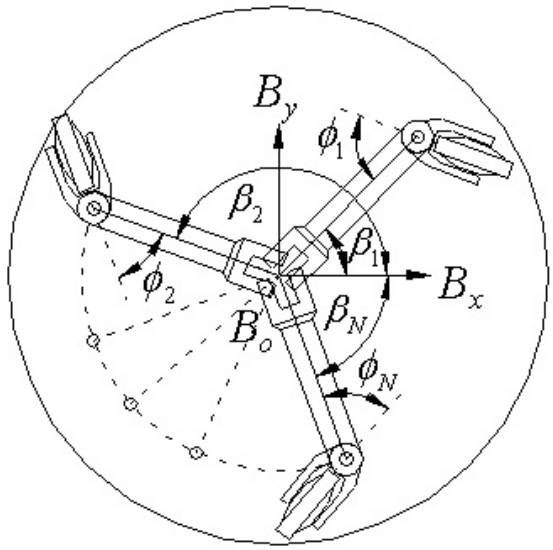

Figure 2: The common frame {B} is attached at the center of the mobile base. All the forward kinematics from each individual wheel module is transform to reflect the end-effector at frame {B}.

The resulting Jacobian for a single wheel module with respect Frame {E} is:

$$^{E}\mathbf{J} = \begin{bmatrix} -bs_{\phi} & rc_{\phi} & 0 \\ bc_{\phi} + h & rs_{\phi} & h \\ 1 & 0 & 1 \end{bmatrix} \tag{5}$$

3 Kinematics of Mobile Base

To find the Jacobian matrices of the rest of the wheels, it is only necessary to express them in the common frame (Frame {B}), which is attached to the center of the mobile base:

$$^{B}\mathbf{J}_i = ^{B}\mathbf{R}_{Ei}.^{Ei}\mathbf{J} \tag{6}$$

where i denotes the caster wheel of interest, N is total number of wheel module in the mobile base and $^{B}\mathbf{R}_{Ei}$ is the rotation matrix derived from angle β, as shown in Figure 2. This results in the Jacobian of wheel i with respect to common Frame {B} at the center of the mobile base:

$$^{B}\mathbf{J}_i = \begin{bmatrix} hs_{\beta_i} + bs_{\beta_i+\phi_i} & rc_{\beta_i+\phi_i} & +hs_{\beta_i} \\ hc_{\beta i} + bc_{\beta i+\phi i} & -rs_{\beta i+\phi i} & hc_{\beta_i} \\ 1 & 0 & 1 \end{bmatrix} \tag{7}$$

and

$$^{B}\mathbf{J}_i^{-1} = \frac{1}{rb} \begin{bmatrix} rs_{\beta_i+\phi_i} & rc_{\beta_i+\phi_i} & -rhc_{\phi_i} \\ bc_{\beta i+\phi i} & -bs_{\beta i+\phi i} & bhs_{\phi_i} \\ -rs_{\beta_i+\phi_i} & -rc_{\beta_i+\phi_i} & r(b + hc_{\phi}) \end{bmatrix} \tag{8}$$

This derivation yields the same result as the geometric approach found in [12] and [14]. Note that the inverse always exists for $rb \neq 0$.

3.1 Implementation Issue: Forward Kinematics

In the expression of the Jacobian matrix (Equation 7), we assume that we are able to obtain the joint variable $\dot{\sigma}$ for the purpose of forward kinematics. In the real application, σ is not measurable.

In the inverse kinematics, however, it is possible to remove the σ component (see Equation 8). The inverse of Jacobian matrix without the σ component for any wheel i is obtained by simply removing the last row of ${}^{B}\mathbf{J}_i^{-1}$.

$$ {}^{B}\mathbf{J}_i^{-1} = \frac{1}{rb} \begin{bmatrix} rs_{\beta_i+\phi_i} & rc_{\beta_i+\phi_i} & -rhc_{\phi_i} \\ bc_{\beta i+\phi i} & -bs_{\beta i+\phi i} & bhs_{\phi_i} \end{bmatrix} \tag{9} $$

which means

$$ \begin{bmatrix} \dot{\rho}_i \\ \dot{\phi}_i \end{bmatrix} = {}^{B}\mathbf{J}_i^{-1} \begin{bmatrix} \dot{x} \\ \dot{y} \\ \dot{\theta} \end{bmatrix} \tag{10} $$

The Jacobian inverse of all the individual wheel modules can be combined to form an augmented Jacobian inverse $\mathbf{J}_{aug}^{-1}$:

$$ \begin{array}{ccc} \begin{bmatrix} \dot{\phi}_1 \\ \dot{\rho}_1 \\ \dot{\phi}_2 \\ \dot{\rho}_2 \\ \dots \\ \dot{\phi}_N \\ \dot{\rho}_N \end{bmatrix} & = & \underbrace{\begin{bmatrix} \mathbf{J}_1^{-1} \\ \\ \mathbf{J}_2^{-1} \\ \\ \dots \\ \mathbf{J}_N^{-1} \\ \\ \end{bmatrix}}_{\mathbf{J}_{aug}^{-1}.} \cdot \begin{bmatrix} \dot{x} \\ \dot{y} \\ \dot{\theta} \end{bmatrix} \\ \dot{\mathbf{q}}_{aug} & = & \qquad\qquad \dot{\mathbf{x}} \end{array} \tag{11} $$

The forward kinematics can be obtained by solving for $(\dot{x}, \dot{y}, \dot{\theta})^T$ from Equation 11, which represents a $2N$ equations with 3 unknowns ($N \geq 2$), for which in general, there may not be a solution. But in this case, the wheel modules are held together by physical constraints:

$$ \begin{bmatrix} \dot{x} \\ \dot{y} \\ \dot{\theta} \end{bmatrix} = \mathbf{J}_1. \begin{bmatrix} \dot{\phi}_1 \\ \dot{\rho}_1 \end{bmatrix} = \mathbf{J}_2. \begin{bmatrix} \dot{\phi}_2 \\ \dot{\rho}_2 \end{bmatrix} = \ldots = \mathbf{J}_N. \begin{bmatrix} \dot{\phi}_N \\ \dot{\rho}_N \end{bmatrix} \tag{12} $$

therefore an exact solution exist using the left pseudo inverse of $\mathbf{J}_{aug}^{-1}$, i.e.:

$$ \mathbf{J}_{LPI} = ((\mathbf{J}_{aug}^{-1})^T.\mathbf{J}_{aug}^{-1})^{-1}.(\mathbf{J}_{aug}^{-1})^T \tag{13} $$

where

$$\begin{bmatrix} \dot{x} \\ \dot{y} \\ \dot{\theta} \end{bmatrix} = \mathbf{J}_{LPI}. \begin{bmatrix} \dot{\phi}_1 \\ \dot{\rho}_1 \\ \dot{\phi}_2 \\ \dot{\rho}_2 \\ \dots \\ \dot{\phi}_N \\ \dot{\rho}_N \end{bmatrix} \tag{14}$$

Note that $\mathbf{J}_{LPI}^{-1}$ always exists for $rb \neq 0$.

When the operational space velocity command vector is obtained from the control law, it can be immediately used in Equation 11 to produce the joint rate command vector to be sent out to the high level controller for each joint to obtain the desired motion.

4 Kinematic Analysis

The aim of kinematic analysis is to determine the optimal design parameters that exert, as much as possible, equal effort in joint space to produce any motion in task space. In a serial manipulator, this is often reflected in a manipulability ellipsoid [16] at the end-effector. This is directly related to the singularity issues whereby the end-effector loses the ability to move in certain direction (the degenerate direction).

In the case of caster wheel in a mobile base system, singularity is not an issue, as it is already shown above Equation 8 that the inverse of the Jacobian matrix always exists, as long as $r \neq 0$ and $b \neq 0$. The exception to this would be when passive joints are included in the system and only 3 joints are actuated to produce motion in 2D plane.

A manipulability ellipsoid, or more appropriately, the *maneuverability ellipsoid*, shows the velocity generated in task space with bounded joint velocities. Please note that it is not appropriate to use the Jacobian matrix in Equation 7, because it still reflects the contribution of the imaginary joint σ. The appropriate analysis should be performed on the $\mathbf{J}^{-1}$ matrix without the contribution of σ (from Equation 9) or the Jacobian matrix obtained from Equation 13.

The joint space of a caster wheel, however, only contains two joints: the steer and the drive and it is obvious that when the mobile base diameter is much larger than the wheel radius, then one rotation in steer angle produces a much larger motion than one revolution of the wheel.

5 Dynamic Modelling

The caster wheel is treated as a serial link manipulator, each subjected to:

$$\boldsymbol{\tau} = \mathbf{A}(\mathbf{q})\ddot{\mathbf{q}} + \mathbf{b}(\mathbf{q}, \dot{\mathbf{q}}) + \mathbf{g}(\mathbf{q}) \tag{15}$$

where $\boldsymbol{\tau}$ is the torque to be sent to joint actuators, $\mathbf{A}$ is the inertia matrix, $\mathbf{b}$ is vector that contains the Coriolis and Centrifugal effects, and $\mathbf{g}$ is the gravitational effect on the joints.

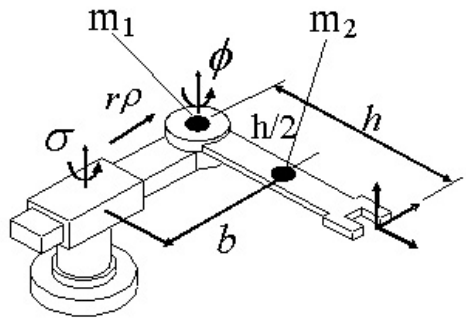

Figure 3: Dynamic model of a wheel module, with three actuators and two centers of mass m_1 and m_2.

The $\mathbf{A}$ matrix is for individual wheel module is derived by:

$$\mathbf{A} = \sum_{i}^{K} m_i \mathbf{J}_{v_i}^T \mathbf{J}_{v_i} + \mathbf{J}_{\omega_i}^T \mathbf{I}_C \mathbf{J}_{\omega_i} \tag{16}$$

where the individual caster wheel is modelled as having a center of masses (m_1 and m_2) (Figure 3) and K is the total number of centres of masses ($K = 2$). The task space kinetic energy matrix $\mathbf{\Lambda}_i$ is obtained for each wheel module i as:

$$\mathbf{\Lambda}_i = ({}^B\mathbf{J}_i \mathbf{A}_i^{-1} . {}^B\mathbf{J}_i^T)^{-1} \tag{17}$$

where ${}^B\mathbf{J}_i$ is a 3×3 matrix of Equation 8.

The combined dynamics of the mobile base at its centre, expressed in Frame {B} is obtained by combining the dynamics of all the individual "serial manipulators" reflected at the end-effector (augmented object model [13] [14]):

$$\mathbf{\Lambda}_{aug}(\mathbf{q}) = \sum_{i=1}^{N} \mathbf{\Lambda}_i(\mathbf{q}) \tag{18}$$

6 Dynamic Analysis

The aim of the analysis is to come up with an optimised set of design parameters so that there will be equal effort in producing motion in all directions. This could be done by analysis the ellipsoid formed by the singular values and singular vectors of the $\mathbf{\Lambda}_{aug}$ matrix, which is the inertia of the mobile base in 2D task space [17]. Since the analysis for translational and rotational motion are to be analysed separately, it is necessary to form separate $\mathbf{\Lambda}$ matrix for translational and rotational motion:

$$\begin{aligned} \mathbf{\Lambda}_{v_i} &= (\mathbf{J}_{v_i} \mathbf{A}_i^{-1} \mathbf{J}_{v_i}^T)^{-1} \\ \mathbf{\Lambda}_{\omega_i} &= (\mathbf{J}_{\omega_i} \mathbf{A}_i^{-1} \mathbf{J}_{\omega_i}^T)^{-1} \end{aligned} \tag{19}$$

where $\mathbf{J}_{v_i}$ is the top two rows of the Jacobian matrix (for translational motion $\dot{x}$ and $\dot{y}$) and $\mathbf{J}_{\omega_i}$ is the bottom row of the Jacobian matrix for orientation ($\dot{\theta}$). It

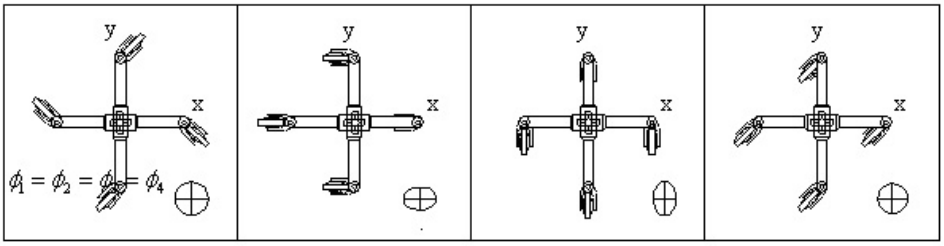

Figure 4: The inertial ellipsoid of $\mathbf{\Lambda}_{v_i}^{-1}$ for translational motion of the combined mobile platform. The major principal axis of the ellipsoid shows the direction that reflects minimum inertia in the motion, hence it is easier to move in those directions.

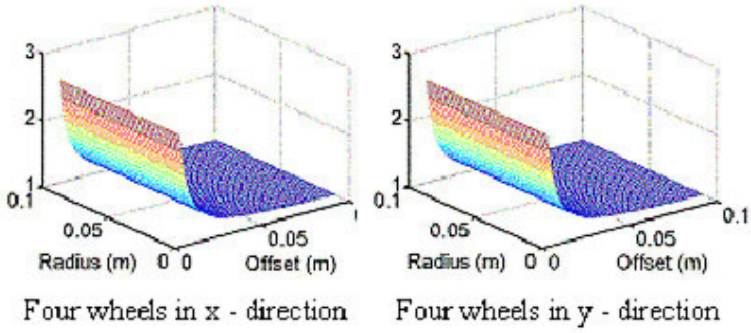

Figure 5: The effect of the design parameters: r and b. Offset of the caster wheel plays a major role below a certain threshold value.

is also possible to perform the analysis on $\mathbf{\Lambda}_{v_i}^{-1}$ and $\mathbf{\Lambda}_{\omega_i}^{-1}$ to avoid performing the extra inversion. An example of the visual representation of the reflected inertia in the 2D planar motion is shown in Figure 4 for translational motion for a mobile base comprised of four sets of wheel module (therefore eight actuated joints).

It is the ideal case when a mobile base is capable of moving in all directions with equal "ease". In this case, the inertial ellipsoid will become a circle. Condition number of $\mathbf{\Lambda}$ can be utilised to show the ratio between the major and minor principal of the ellipsoids. A condition number of 1 means that the major and minor principal axes are of the same length.

Figure 5 shows the plot of condition numbers of the combined mobile base (with 4 wheel modules) for various values of radius and offset of the wheel. It is shown that the wheel offset plays a major role below a certain threshold value. The result was produced with example values of $h = 0.325m$ (radius of the mobile platform), $m_1 = 1$kg for each of the wheels, and $m_2 = 50$kg for each of the wheel module.

Our dynamic analysis shows that dynamic isotropic configurations can be achieved when identical powered caster wheels (identical $\mathbf{\Lambda}$) are distributed in a polar symmetric configuration around the centre of the base. Mathematical proof will be shown in future paper, but we show some numerical results here. Figure 6 shows

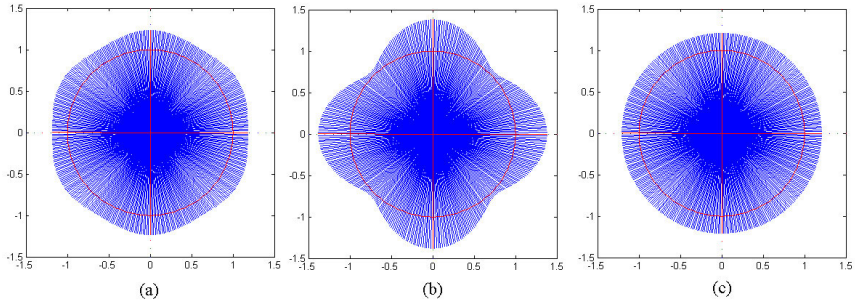

Figure 6: The effect of number of identical wheels on the condition number of $\mathbf{\Lambda}$ as a function of steering angle ϕ for translational motion (therefore all wheels faces the same direction). The result is shown for mobile base with (a)3 wheel (b)four wheel (c)five wheel configurations distributed in polar symmetry.

the condition numbers of $\mathbf{\Lambda}$ in polar plot as a function of steering angle ϕ. The polar angle is the steering angle ϕ and the radial length is the condition number of $\mathbf{\Lambda}$. A good design would be one where condition number is close to 1 for all steering angle. The circle with radius 1 represents the condition number of 1. The figure shows dependency of the condition number on steering angle, with the 5 wheel configuration showing least dependency. It is also interesting to note that the four wheel configuration achieves condition number 1 only at $\pm 45^o$, and $\pm 135^o$, although the condition number changes more for different steering angles. This plot could be used as a tool for designing a mobile base to achieve isotropic effect with different design parameters.

7 Conclusion

This paper presents the kinematics and dynamics of a mobile platform. It models each wheel module as a serial manipulator, where all the serial manipulators have a common operational point, which is attached at the center of the mobile platform. Dynamic analysis was performed to determine the effect of the design parameters on the maneuverability of the mobile platform. It was found that an optimal length of offset for the caster wheel was essential so that motion in all direction can be produced with equal effort.

References

[1] P. Muir and C. P. Newman, "Kinematic modelling of wheeled mobile robots," *Journal of Robotic Systems*, vol. 4, no. 2, pp. 281–340, 1987.

[2] S. Ostrovskaya, J. Angeles, and R. Spiteri, "Dynamics of a mobile robot with three ball-wheels," *The International journal of Robotics Research*, vol. 19, no. 3, pp. 1–11, 2000.

[3] W. M and H. Asada, "Design and control of ball wheel omnidirectional vehicles," *Proc. Intl. Conf. Robotics and Automation*, pp. 153–161, 1995.

[4] L. Ferriere, B. Raucent, and G. Campion, "Design of omnidirectional robot wheels," *Proc. Intl. Conf. on Robotics and Automation*, vol. 4, pp. 3664–3670, 1996.

[5] W. La, T. Koogle, D. L. Jaffe, and L. Leifer, "Toward total mobility: an omnidirectional wheelchair," *Proc. 4th RESNA*, pp. 75–77, 1981.

[6] I. Paromtchik and U. Rembold, "Practical approach to motion generation and control for an omnidirectional mobile robot," *Proc. IEEE Intl. Conf. Robotics and Automation*, vol. 4, pp. 2790–2795, 1994.

[7] J. Alexander and J. Maddocks, "On the kinematics of wheeled mobile robots," *The International Journal of Robotics Research*, vol. 8, no. 5, pp. 15–27, 1989.

[8] S. Ostrovskaya, J. Angeles, and R. Spiteri, "Nonholonomic sysmtes revisited within the framework of analytical mechanisms," *Appl Mech Rev*, vol. 51, no. 7, pp. 415–433, 1998.

[9] M. Wada and S. Mori, "Holonomic and omnidirectional vehicle with conventional tires," *Proc. IEEE Intl. Conf. Robotics and Automation*, vol. 1, pp. 265–270, 1996.

[10] L. Ferriere, B. Raucent, and A. Fournier, "Design of a mobile robot equipped with off-centered orientable wheels," *Proc. of the Research Workshop of ERNET*, pp. 127–136, 1996.

[11] G. Campion, G. Bastin, and B. D'Andrea-novel, "Structural properties and clasification of kinematic and dynamic models of wheeled mobile robots," *IEEE Transactions on Robotics and Automation*, vol. 12, pp. 47–62, February 1996.

[12] B.-J. Yi and W.-K. Kim, "The kinematics for redundantly actuated omnidirectional mobile robots," *Journal of Robotic Systems*, vol. 19, no. 6, pp. 255–267, 2002.

[13] O. Khatib, "A unified approach for motion and force control of robot manipulators: The operational space formulation," *IEEE J. Robotics and Automation*, vol. RA-3, no. 1, pp. 43–53, 1987.

[14] R. Holmberg, "Design and development of powered-caseter holonomic mobile robots." PhD. Dissertation, August 2000. Stanford University.

[15] D. Williams and O. Khatib, "The virtual linkage: A model for internal forces in multi-grasp manipulation," *Proc. IEEE International Conference on robotics and Automation*, vol. 3, pp. 1025–1030, 1993.

[16] T. Yoshikawa, "Manipulability of robotic mechanisms," *Intl. J. Robotics Research*, vol. 4, pp. 3–9, Summer 1985.

[17] H. Asada, "A geometrical representation of manipulator dynamics and its application to arm design," *Trans ASME, J. Dyn. Syst., Meas and Control,*, vol. 105, pp. 131–135, 1983.